BIOCHEMISTRY
including biophysical chemistry & molecular biology

Article

pubs.acs.org/biochemistry

Photoconversion Mechanism of the Second GAF Domain of Cyanobacteriochrome AnPixJ and the Cofactor Structure of Its Green-Absorbing State

Francisco Velazquez Escobar,[†] Tillmann Utesch,[†] Rei Narikawa,[‡,§] Masahiko Ikeuchi,[‡,∥] Maria Andrea Mroginski,[†] Wolfgang Gärtner,[⊥] and Peter Hildebrandt*[,†]

[†]Institut für Chemie, Technische Universität Berlin, Sekr. PC14, Straße des 17 Juni 135, D-10623 Berlin, Germany

[‡]Department of Life Sciences (Biology), Graduate School of Art and Sciences, University of Tokyo, Komaba, Meguro, Tokyo 153-8902, Japan

[§]Japan Science and Technology Agency (JST), PRESTO, 4-1-8 Honcho Kawaguchi, Saitama 332-0012, Japan

[∥]Japan Science and Technology Agency (JST), CREST, 4-1-8 Honcho Kawaguchi, Saitama 332-0012, Japan

[⊥]Max-Planck-Institut für Chemische Energiekonversion, Stiftstrasse 34-36, D-45470 Mülheim an der Ruhr, Germany

Supporting Information

ABSTRACT: Cyanobacteriochromes are members of the phytochrome superfamily. In contrast to classical phytochromes, these small photosensors display a considerable variability of electronic absorption maxima. We have studied the light-induced conversions of the second GAF domain of AnPixJ, AnPixJg2, a phycocyanobilin-binding protein from the cyanobacterium *Anabaena* PCC 7120, using low-temperature resonance Raman spectroscopy combined with molecular dynamics simulations. AnPixJg2 is formed biosynthetically as a red-absorbing form (Pr) and can be photoconverted into a green-absorbing form (Pg). Forward and backward phototransformations involve the same reaction sequences and intermediates of similar cofactor structures as the corresponding processes in canonical phytochromes, including a transient cofactor deprotonation. Whereas the cofactor of the Pr state shows far-reaching similarities to the Pr states of classical phytochromes, the Pg form displays significant upshifts of the methine bridge stretching frequencies concomitant to the hypsochromically shifted absorption maximum. However, the cofactor in Pg is protonated and adopts a conformation very similar to the Pfr state of classical phytochromes. The spectral differences are probably related to an increased solvent accessibility of the chromophore which may reduce the π-electron delocalization in the phycocyanobilin and thus raise the energies of the first electronic transition and the methine bridge stretching modes. Molecular dynamics simulations suggest that the $Z \rightarrow E$ photoisomerization of the chromophore at the $C{-}D$ methine bridge alters the interactions with the nearby Trp90 which in turn may act as a gate, allowing the influx of water molecules into the chromophore pocket. Such a mechanism of color tuning AnPixJg2 is unique among the cyanobacteriochromes studied so far.

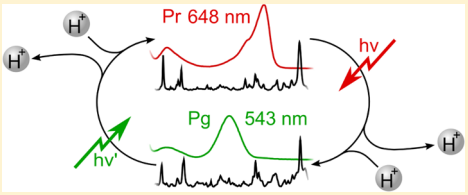

Bilin-binding photosensory pigments have long been synonymous with the red/far-red light-sensing phytochrome photoreceptors of higher and lower plants.[1,2] An outstandingly large number of experiments clearly have documented the paramount role of phytochromes in photomorphogenesis.[3−6] These photochromic photoreceptors comprise a small protein family (e.g., phyA−phyE in *Arabidopsis thaliana*) that can be switched between two thermally stable or long-lived states by irradiation with light of appropriate wavelengths. In "classical" phytochromes, the red light-absorbing form (Pr) shows an absorbance maximum at 667 nm (phyA of oat), and the far red-absorbing form (Pfr) absorbs at 730 nm. Also, the kinetics of the photoinduced reaction cycle has been studied intensively and in molecular detail.[7−13]

Unexpectedly, genome sequencing has unravelled a much wider distribution of phytochromes in prokaryotes. Initially, phytochromes were identified in cyanobacteria showing the canonical structure of plant phytochromes,[14] rapidly followed by demonstration of the presence of functional phytochromes also in nonphotosynthetic bacteria and even in fungi.[15] Ongoing research revealed phytochromes with altered chromophore structures and also identified phytochromes with a modified photochemistry. One class of these novel phytochromes possesses a thermally stable Pfr state that is photoconverted to the hypsochromic Pr state (bathy phytochromes), which in classical or prototypical phytochromes represent the stable dark state.[16] However, in prototypical and bathy phytochromes, the chromophore structural changes are likely to be very similar, i.e., a *ZZZssa* and *ZZEssa* configuration of the tetrapyrrole chromophore in the Pr and Pfr state, respectively.

Received: April 23, 2013
Revised: June 7, 2013
Published: June 28, 2013

   dx.doi.org/10.1021/bi400506a | *Biochemistry* 2013, 52, 4871−4880

In contrast, cyanobacterial bilin-binding proteins were identified that exhibit remarkable variations of the classical phytochrome blueprint. These novel cyanobacteriochromes (CBCRs) are composed in many cases as multi-GAF domain proteins.[17] This architecture is unexpected as the lyase activity (autocatalytic chromophore binding) and the photochemistry are often maintained by a single, isolated GAF domain, in contrast to orthodox phytochromes, where three domains (PAS, GAF, and PHY domains) provide the lyase activity and establish the spectroscopic properties.[18,19]

Despite a growing number of reports on their absorbance maxima variation and some information on their biological role in cyanobacteria,[20] little is known about the molecular mechanisms of the two-state conversion of CBCRs, and the few studies on the chromophore conformation and its structural changes during the light-driven photoprocess have led to partially controversial conclusions.[20−25] One of the most remarkable properties is the variability of the electronic absorption of the parent states, ranging from the red to the near-UV spectral region, which is quite a contrast to the color change between 660 and 700 nm in classical phytochromes.[18−23] Previous studies have shown that CBCRs employ different strategies for controlling the electronic absorption, for instance via interrupting the delocalized π-electron system by addition of a cysteine thiol function to the central methine bridge[21−23] or by deprotonation of the tetrapyrrole chromophore.[17]

Resonance Raman (RR) spectroscopy can provide detailed insight into the chromophore structure in photoreceptors, especially when combined with theoretical methods. This approach had been proven successful for canonical phytochromes.[13,26,27] On the basis of the knowledge obtained from plant and canonical cyanobacterial phytochromes, we present here the first RR study of an isolated GAF domain from a CBCR. Complemented by molecular dynamics (MD) simulations, we analyzed in detail the conformational changes of the second GAF domain of AnPixJ from *Anabaena* sp. PCC 7120 (AnPixJg2). In addition to identifying the chromophore conformations in the stable parent states (Pr and Pg), we determined the chromophore structure of two intermediates by low-temperature RR spectroscopy.

Absorption properties and the physiological relevance of this CBCR, such as phototaxis and bilin expression, were reported by Narikawa et al.,[28] and very recently, the crystal structure of the parent red-absorbing state Pr (λ_{max} = 648 nm) has been described.[29] In addition, the dynamics of the photoconversions between the Pr state and the green-absorbing form Pg (λ_{max} = 543 nm) were studied by time-resolved optical spectroscopies,[30] thus making AnPixJg2 an excellent model for analyzing, on a molecular basis, the mechanism of the photoconversion of CBCRs and the color tuning of the parent states.

EXPERIMENTAL PROCEDURES

Sample Preparation. AnPixJg2 was heterologously expressed in phycocyanobilin (PCB)-producing *Escherichia coli* and purified as holoprotein including PCB as described elsewhere.[28] Sample preparation and measurements were performed under green light using LEDs at 515 nm. Buffer solutions (H_2O/D_2O Tris buffer, 50 mM Tris, 300 mM NaCl, 5 mM EDTA, pH/pD 7.8) were prepared with chemicals of the highest purity available (see Supporting Information). Protein samples were dialyzed in a microcon filter by centrifugation up to a concentration corresponding to an optical density of 30 at the chromophore absorption band.

Raman Experiments. Measurements were carried out with a Bruker FT Raman spectrometer RFS 100/S (Nd:YAG cw laser, 1064 nm, line width 1 cm^{-1}), equipped with a nitrogen-cooled cryostat (Resultec-Linkam). All Raman spectra were recorded at −140 °C. The laser power at the sample was kept at 780 mW with a laser focus diameter of ca. 100 μm. Possible laser-induced damage of the phytochrome samples was controlled by comparing the spectra obtained before and after a series of measurements; no such degradation was observed. For each spectrum the accumulation time was 1 h. Spectra of the Pr state were collected after a 2 min irradiation at 530 nm (LED) at 20 °C, whereas the spectra of the Pg state were obtained after illumination at 660 nm under otherwise the same conditions. This irradiation protocol yielded accumulation of the respective state with only negligible contributions of the other parent state species. For the intermediate states, the following cryogenic trapping procedure was used. The starting point was the sample exposed to green light which mainly contained the Pr state and only very small contributions from the Pg state. Subsequent to the Raman measurement at −140 °C, the sample was irradiated at stepwise increasing temperatures above −140 °C with 660 nm for 10 min and cooled to −140 °C again to measure the Raman spectrum. The analogous procedure was applied to trap the intermediates of the Pg-to-Pr conversion using green light irradiation. Details of the measuring protocol are given in the Supporting Information (Table S1). The component spectra of the pure parent states could readily be obtained from the experimental spectra measured from the samples irradiated with green or red light via mutual subtraction to remove minor contributions of the Pg or Pr state, respectively. Obtaining the spectra of the pure intermediates from the raw spectra measured from samples after irradiation at specific trapping temperatures required iterative subtraction procedures as not only the target intermediate but also the precursor and the thermal relaxation product might contribute to the experimental spectrum. Details of the subtraction procedure are given in the Supporting Information (Table S2).

Molecular Dynamics Simulations. The structural models for the Pr and Pg states of AnPixJg2 cyanobacteriochrome, used for atomistic MD simulations, were constructed using as initial coordinates the crystallographic structure of AnPixJg2 (PDB entry 3W2Z).[29] In the case of the Pr state, the conformation of the PCB chromophore was taken as observed in the crystal structure while initial models for the chromophore in the Pg state were obtained by rotating the C=C bond at the methine bridge between rings *C* and *D* (*C*−*D*) by 155°, 175°, and 195°. The protonation states of all titratable amino acid side chains were set according to pH 7.0. In the case of histidines, the protonation state was adjusted according to their immediate environment. In particular, His94, His119, and His123 in the chromophore binding pocket were protonated at Nε, Nδ, and both nitrogen atoms, respectively. All model systems were solvated in a box of ca. 23000 explicit TIP3P water molecules including 50 mM NaCl.[31]

Prior to the MD simulations, the model systems were prepared by an energy minimization of 20000 steps using the conjugated gradient integrator followed by heating to 300 K. During these steps, all heavy atoms were restrained to their positions by applying a force of 25 kcal mol^{-1} $Å^{-2}$). These restraints, including those of the chromophore for the Pr

model, were stepwise removed during the solvent equilibration within 60 ps. For the Pg models, these last steps together with a subsequent 5 ns MD simulation step were performed keeping the chromophore fixed to adapt the protein environment to the new conformation of the photoproduct. The models for the Pr state and the photoproducts were then thermally equilibrated at 300 K for 5 and 15 ns, respectively.

While the structures of the Pg models built with initial C−C═C−N(*D*) dihedral angles of 155° and 175° converged to a PCB geometry characterized by a strongly distorted torsional angle N(*C*)−C···C−N(*D*) angle of ca. 105°, the structural model constructed with an initial C−C═C−N(*D*) dihedral angle of 195° slowly evolved to a structure characterized by the *ZZZssa* conformation of the PCB chromophore as found in the Pr state (Supporting Information, Figures S6 and S7). Accordingly, we will refer to these structural models as Pg155, Pg175, and Pr195. Given the high similarity with the original X-ray-based Pr model, the engineered Pr195 model was not considered for further discussions. The MD simulations were carried out with NAMD 2.7[32] using the CHARMM 27 force field[33] with an extension for the PCB chromophore derived by Kaminski et al.[34] During these simulations, the number of particles (*N*), the pressure (*P*), and the temperature (*T*) were kept constant using the Langevin piston method.[35] Short-range electrostatics and van der Waals interactions in the periodic systems were calculated with a simple cutoff at 12 Å, whereas long-range electrostatics were determined with the particle Ewald summation.[36] To enable a time step of 2 fs, all bonds containing hydrogen atoms were frozen with the SHAKE algorithms.[37] The solvent accessible area of the chromophore was evaluated with VMD1.8.7[38] every 25 ps, assuming a radius of 1.4 Å for a water molecule.

RESULTS AND DISCUSSION

Despite the large separation of the excitation line (1064 nm) from the first electronic transition of the chromophore of the Pr state (660 nm), the measured Raman spectra are dominated by the preresonantly enhanced Raman bands of the bilin cofactor and thus are referred to as resonance Raman (RR) spectra. This is also true for the Pg state, although its electronic transition is even further blue shifted to ca. 560 nm. There are only small although clearly detectable contributions from nonresonance Raman bands of the protein matrix such as the methyl and methylene deformation modes of amino acid side chains (ca. 1450 cm^{-1}) and the amide I modes of the polypeptide backbone (ca. 1650 cm^{-1}) (Figure 1). These poorly structured features partially overlap with the RR bands of the cofactor. In addition, there is a relatively sharp band at 1003 cm^{-1} which is due to the ring-breathing mode of phenylalanine residues. The intensity of this band can be used as an internal standard to estimate the relative resonance enhancement for the cofactor Raman bands of the various states of AnPixJg2. In accordance with the poorer resonance conditions for Pg, we have found, on average, that the enhancement for this state is 2-fold weaker than for Pr. Even lower resonance enhancements and thus relatively strong contributions from the protein Raman bands are noted for the intermediate states including a deprotonated chromophore (vide infra).

Resonance Raman Spectroscopy of the Pr State. The overall vibrational band pattern of the parent state Pr displays far-reaching similarities with that of the Pr states of canonical phytochromes carrying a PCB chromophore as exemplified for the PCB adduct of plant phytochrome phyA (Figure 1A,B). A very good agreement is noted for the bands in the C═C stretching region between 1500 and 1700 cm^{-1} which are sensitive marker bands for the conformation of PCB and in particular for the methine bridge configuration. This finding is in agreement with the crystal structure data indicating that the chromophore in the Pr state of AnPixJg2 adopts a *ZZZssa* configuration as in the case of phyA(PCB) and Cph1Δ2 (Figure 2).[27,29,39,40] Adopting the vibrational assignment from the analysis of the RR spectra of phyA-PCB, the dominant band at 1635 cm^{-1} is attributed to the C═C stretching of the *C*−*D* methine bridge (*C*−*D* stretching), whereas the weak shoulder on the lower-frequency side at 1607 cm^{-1} is attributed to the *B*−*C* stretching (Figure 1A,B and Supporting Information, Figure S1; see Figure 2 for the structural formula of the cofactor). The corresponding *A*−*B* stretching mode is likely to be hidden under the high-frequency wing of the 1635 cm^{-1} band. Furthermore, this spectral region includes the in-phase N−H in-plane bending (ip) mode of the ring *B* and *C* nitrogen atoms at 1576 cm^{-1} (phyA-PCB) which is a characteristic marker for the protonation of the cofactor. In fact, the RR spectrum of the Pr state of AnPixJg2 shows a band at a very similar position (1579 cm^{-1}) which disappears upon H/D exchange (Figure 1A,B and Supporting Information, Figure S1). The corresponding N−D ip mode is assigned to a weak band at 1076 cm^{-1} (Supporting Information, Figure S2) analogous to previous findings for phyA-PCB.[41] Also, the other isotopic shifts brought about by H/D exchange are similar in

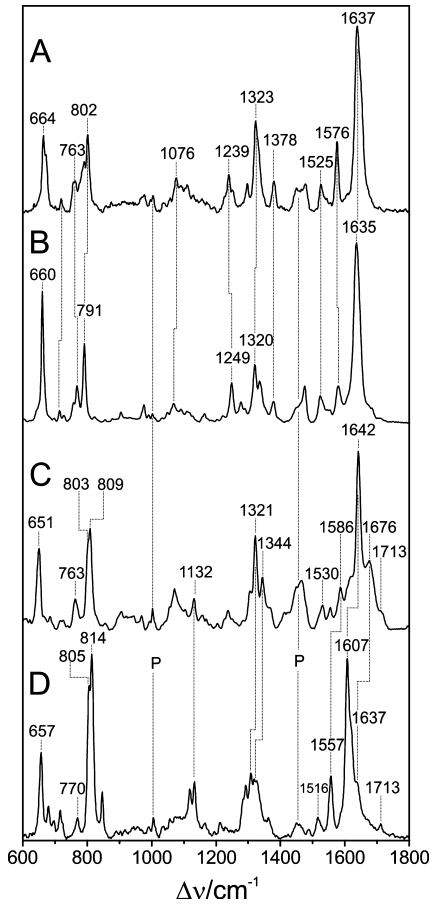

Figure 1. Overview RR spectra of the parent states of AnPixJg2 and the 65 kDa fragment phyA reconstituted with PCB, measured in H_2O at pH 7.8. A, Pr of phyA-PCB; B, Pr of AnPixJg2; C, Pg of AnPixJg2; and D, Pfr of phyA-PCB.

dx.doi.org/10.1021/bi400506a | *Biochemistry* 2013, 52, 4871−4880

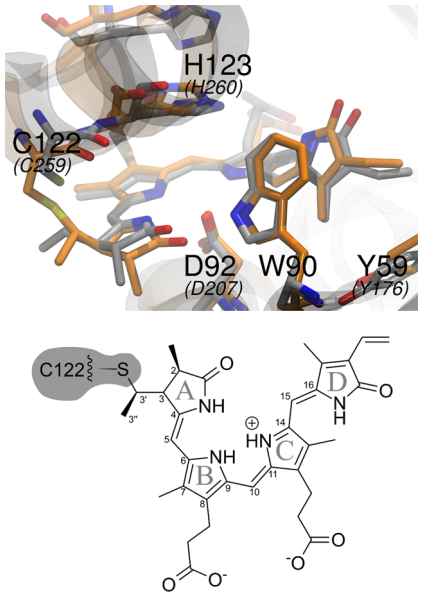

Figure 2. (Top panel) Chromophore binding pocket of AnPixJg2 in the Pr state. The crystal structure is represented in gray carbon atoms. The structure obtained after the MD trajectory is displayed in orange. Structural alignment of both (crystal and MD) coordinates refers to the lowest RMSD of the PCB chromophore coordinates. AnPixJg2 specific amino residues are indicated with normal character style, whereas corresponding residues of Cph1Δ2 are presented in italics. (Bottom panel) Structural formula of the PCB chromophore in the *ZZZssa* configuration.

the Pr states of AnPixJg2 and phyA-PCB, which not only is consistent with the cationic cofactor structure (all four ring nitrogens being protonated) but also supports the assignments discussed above.

Only details of the cofactor structure and its interactions with the protein environment seem to be different for the Pr state of AnPixJg2, compared to those of the Pr state of canonical PCB-binding phytochromes. Spectral differences in the region between 600 and 850 cm^{-1} mainly result from torsional and deformation modes of rings *C* and *D* (at ca. 650 cm^{-1}) and from C−H out-of-plane deformation (HOOP) modes of the *C*−*D* methine bridge, pointing to structural variations specifically in this part of the cofactor (Figure 1A,B). In fact, the crystallographic data for the Pr state of AnPixJg2 indicate a torsional angle around the *C*−*D* methine bridge that is distinctly larger (27°) than that found for Cph1Δ2 (2°).[27,29,39] It is also larger than that of the structural model for phyA-PCB (11°).[40] One of the most striking differences between the crystallographic data for the Pr states of AnPixJg2 and canonical phytochromes refers to the hydrogen bond interactions of the pyrrole rings. In canonical phytochromes, the ring *B* and *C* N−H groups interact with a structural water (pyrrole water) which in turn forms a hydrogen bond to the backbone carbonyl function of the highly conserved Asp in canonical phytochromes (Asp207 in Cph1Δ2).[39] In AnPixJg2, however, no pyrrole water is detected in the crystal structure, and the carboxylate side chain of this conserved aspartate residue (Asp92 in the AnPixJg2 sequence) forms hydrogen bonds directly with the N−H groups of rings *B* and *C* (Figure 2).[29] MD simulations confirm this picture, although a water molecule enters the chromophore pocket after ca. 2.5 ns. This water molecule, however, remains above the tetrapyrrole plane without interfering with the ring *B*/*C*−Asp92 interactions (Wat1 in Supporting Information, Figure S9).

Resonance Raman Spectroscopy of the Pg State. The most remarkable observation refers to the RR bands in the region between 1500 and 1700 cm^{-1}, which, at first glance, seem to differ substantially from the RR spectra of Pfr states of canonical phytochromes (Figures 1C,D and 3). The deviations,

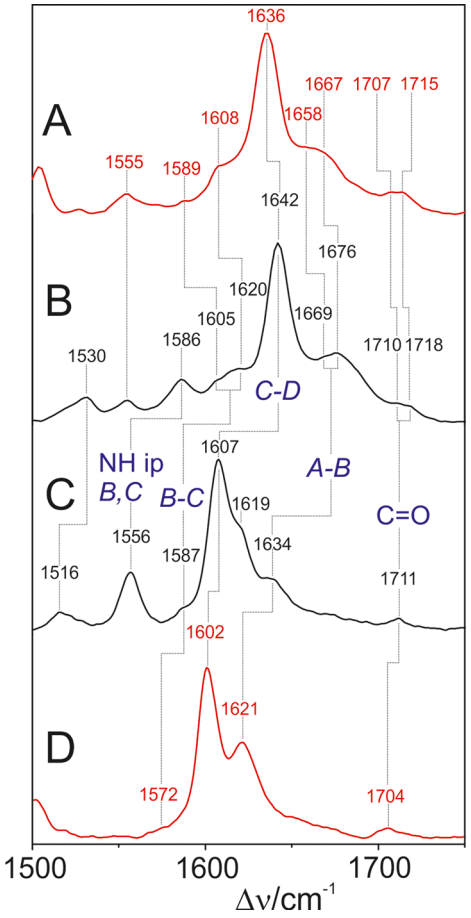

Figure 3. Expanded view of the RR spectra in the C=C stretching region of the Pg state of AnPixJg2 and the Pfr state of the 65 kDa fragment phyA reconstituted with PCB, measured at pH/pD 7.8. A, Pg of AnPixJg2 in D_2O; B, Pg of AnPixJg2 in H_2O; C, Pfr of phyA-PCB in H_2O; and D, Pfr of phyA-PCB in D_2O. Blue letters indicate the main character of the normal modes involved. Italic letters *A*, *B*, *C*, and *D* refer to the individual pyrrole ring as defined in Figures 2 and 4, and *A*−*B*, *B*−*C*, and *C*−*D* denote the C=C stretchings of the methine bridges between the respective rings. The C=O stretchings of rings *A* and *D* and the N−H in-plane bending of rings *B* and *C* are abbreviated "C=O" and "NH ip *B*,*C*", respectively.

however, are systematic. On the basis of the relative band intensities and the H/D effects one may identify the conjugate band pairs in the RR spectra of Pg (AnPixJ) and Pfr (phyA-PCB), indicating that nearly all of the Pg modes in this region are upshifted by more than 30 cm^{-1}, including the C=C stretching modes of the *C*−*D*, *A*−*B*, and *B*−*C* methine bridges at 1642, 1676, and 1620 cm^{-1}, respectively. This finding implies that all methine bridge modes of the cofactor are found in the RR spectrum of Pg. Thus, we can safely rule out that the blue-shifted absorption maximum in the Pg state is due to the reduction of the *A*−*B* methine bridge double bond such as is the case in the Pg form of TePixJ or in phycoviolobilin, which

dx.doi.org/10.1021/bi400506a | *Biochemistry* 2013, 52, 4871−4880

in turn would afford quite different RR spectra.[21] Furthermore, also the possibility of a deprotonation of the tetrapyrrole cofactor can be ruled out because the RR spectrum of the Pg state of AnPixJg2 shows the N−H ip mode of rings *B* and *C* at 1586 cm^{-1} which disappears in D_2O. The corresponding N−D ip mode is found at 1089 cm^{-1} (Supporting Information, Figure S2). Like the methine stretching modes, the N−H ip mode is upshifted by ca. 30 cm^{-1} compared to Pfr of phyA-PCB. A smaller upshift (14 cm^{-1}) is noted for the other mode involving the N−H ip coordinates of rings *B* and *C* (1530 cm^{-1}) (Figures 1C,D and 3).

Previous cofactor extraction experiments with the denatured protein have revealed a PCB cofactor with a *Z* or *E* configuration of the *C*−*D* methine bridge in the Pr or Pg state, respectively (Figure 4).[28] Whereas the good RR

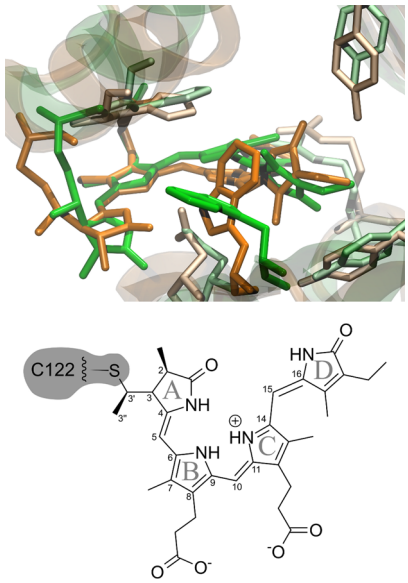

Figure 4. (Top panel) MD equilibrated structure before (orange) and after (green) *Z*/*E* isomerization of the *C*−*D* double bond. (Bottom panel) Structural formula of the PCB chromophore in the *ZZEssa* configuration.

spectroscopic agreement between the Pr states of AnPixJg2 and phyA-PCB points to very similar cofactor structures, it remains to be analyzed if—in addition to the *Z*/*E* isomerization of the *C*−*D* methine bridge—there are further structural changes of the chromophore in the Pg state that are different from those in canonical phytochromes. In this respect, we first focus on the high-frequency region (Figure 3). Compared to the Pfr state of phyA-PCB, we note a significant band broadening of the features above and below the prominent 1642 cm^{-1} band (*C*−*D* stretching). Moreover, a closer inspection reveals asymmetric band shapes indicating, in each case, the involvement of at least two band components. Thus, the minimum number of bands in the C=C stretching region (1590−1680 cm^{-1}) is five, which exceeds the number of Raman-active normal modes (three) and even of the total number of normal modes (four) calculated for PCB, regardless of the specific tetrapyrrole configuration and conformation.[42,43] Furthermore, the similar H/D sensitivity of the band components at 1676 (−9) and 1669 (−11) cm^{-1} suggests that the underlying modes have the same character, i.e., they are dominated by the *A*−*B* stretching coordinate. Correspondingly, the band components at 1620 (−12) and 1605 (−16) cm^{-1} are assigned to modes of mainly *B*−*C* stretching character with the admixture of the *A*−*B* stretching coordinate.[42] These findings indicate that the Pg form exists in two substates differing in terms of the *A*−*B* methine bridge conformation. In this respect, we like to refer to a comparative spectroscopic−theoretical analysis of the Pfr state of biliverdin-binding phytochromes demonstrating, for prototypical but not for bathy phytochromes, conformational equilibria associated with structural changes at the *A*−*B* and *C*−*D* methine bridges.[44] This conclusion was derived not only from the analysis of the methine bridge stretching modes but also from the prominent HOOP mode of the *C*−*D* methine bridge at ca. 810 cm^{-1} that gives rise to two band components. A similar band pattern is also observed in the present RR spectra (Figure 1C,D; more clearly shown in Supporting Information, Figure S3) suggesting that for the Pg state of AnPixJg2 as well as for the Pfr state of phyA-PCB the structural heterogeneity involves the *C*−*D* methine bridge.

Alterations of the hydrogen bond network associated with the structural changes in the chromophore binding pocket are presumably responsible for the spectral deviations between the Pg and Pfr RR spectra in the region between 1200 and 1400 cm^{-1} as it includes modes involving the N−H ip coordinates of rings *A* and *D* and coordinates of the propionate side chains of rings *B* and *C*. Thus, these modes are expected to respond sensitively to structural changes of the immediate protein environment.

Because of the lack of structural data on the Pg state of AnPixJg2 or the Pfr state of any PCB-binding phytochrome, it is not possible to identify particularly important amino acid residues interacting with the tetrapyrrole. However, it is tempting to assume that Trp90 plays a role in controlling the spectral and structural properties of the cofactor because this residue is found in close proximity to ring *D* in the crystal structure of the Pr state of AnPixJg2.[29] Moreover, this residue is conserved only among the red/green-absorbing cyanobacteriochrome subfamily, suggesting a crucial and unique role in the chromophore−Trp90 interaction. In contrast, this aromatic residue is absent in canonical phytochrome sequences. Position 90 in the AnPixJg2 sequence corresponds to the residue 205 in Cph1 or residue 270 in the phyA sequence, located two amino acids below the canonical DIP motif.[45]

Molecular Dynamics Simulations of a Pg Model. Starting with the crystal structure coordinates, we have therefore carried out MD simulations which revealed only slight deviations in the surrounding protein matrix (Figure 2). Specifically Trp90 remained at a distance of 4.1 ± 0.3 Å to ring *D* within a nearly coplanar orientation (169.9 ± 5.7°), underpinning its important role in stabilizing the chromophore in the Pr state. To assess the consequences of the *Z*/*E* isomerization of the *C*−*D* methine bridge on the cofactor protein interactions, two Pg models were constructed, namely the Pg155 model and the Pg175 model (vide supra). As a consequence of the MD simulations, the chromophore in both structural models was found to adopt a distorted albeit stable *ZZEssa* geometry (Figure 4 and Supporting Information, Figure S6 and Table S4), while the overall structure of the protein did not change significantly. Specifically, there were only subtle adjustments of the protein in the vicinity of the cofactor, except for a repositioning of Trp90 and Asp92 (Figure 4). Although these results have to be considered with caution in view of the mechanical force fields for both the protein and the cofactor, they suggest that the *C*−*D* methine bridge isomerization is

dx.doi.org/10.1021/bi400506a | *Biochemistry* 2013, 52, 4871−4880

associated with a distinct weakening of the interactions between ring *D* and Trp90, as reflected by the increased separation (7.6 ± 1.0 Å for Pg155 and 7.3 ± 1.1 Å for Pg175) while maintaining a nearly coplanar orientation. Concomitant to the movement of Trp90, Asp92 is displaced toward ring *A* at the expense of the hydrogen bond interactions with rings *B* and *C*. This reorientation of Asp92 and Trp90 may increase the flexibility of the chromophore in the binding pocket, which in turn provides an explanation for the structural heterogeneity of the tetrapyrrole as reflected by the additional RR bands in the C=C stretching and HOOP regions.

In addition, the structural water contents in the Pr and the "photoproduct" model differ considerably. After the MD simulations, we found 7 solvent molecules in the chromophore binding pocket for the Pr state (in contrast to only 3 H_2O molecules in the crystal structure) and 14 (Pg155) or 11 (Pg175) water molecules for the "photoproduct" (Supporting Information, Figure S10). The increased number of water molecules in the chromophore pocket for the "photoproduct" is mainly the consequence of the reorganization of Trp90 during the MD simulation. Trp90 acts as a kind of gate and opens the chromophore pocket to water molecules when aligning its ring structure parallel to ring *D* of the chromophore. This putative gating mechanism does not affect the protein backbone structure. Only the rearrangement of the protein side chain of Trp90 leads to an increased solvent accessible area of the chromophore for the "photoproduct". The MD simulations showed a significant increase of the solvent accessibility of the chromophore for the "photoproduct" (246.5 ± 16 Å^2 for Pg155 and 246.3 ± 14 Å^2 for Pg175) compared to that of the Pr state (187 ± 12 Å^2) which was evaluated over the last 2 ns of the respective production runs (Supporting Information, Figure S8). Thus, the present MD simulations indicate that the double bond isomerization may cause, in principle, quite substantial alterations in the protein−cofactor interactions even though an accurate analysis of these interactions is possible only on the basis of a crystallographic structure.

Resonance Raman Spectroscopy of the Photoinduced Reaction Cycle. For the Pr → Pg phototransformation, three different intermediates were identified on the basis of the RR spectra at trapping temperatures indicated in Figure 5 (more

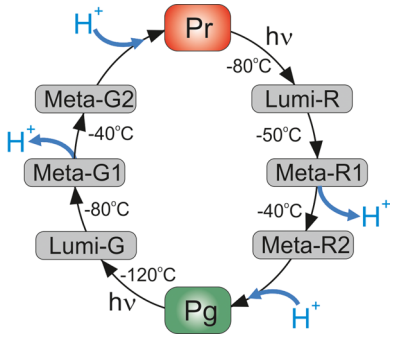

Figure 5. Photoinduced reaction cycle of AnPixJg2.

details are given in the Supporting Information). Unlike canonical phytochromes, where the photochemistry can be initiated even at −140 °C,[41] a red-light-induced photoconversion of AnPixJg2 was observed only above −80 °C, which is in accordance with the relatively slow kinetics determined by transient absorption spectroscopy for the Lumi-R (= $R1_{650-80}$) formation (<100 ns).[30] In this reaction step, the primary *Z*/*E* double bond isomerization at the *C*−*D* methine bridge takes place leading to a red shift of the absorption maximum.[28,30,46] The corresponding cryogenically trapped intermediate displays some features reminiscent of the RR spectrum of the Lumi-R state of phyA (Figure 6B).

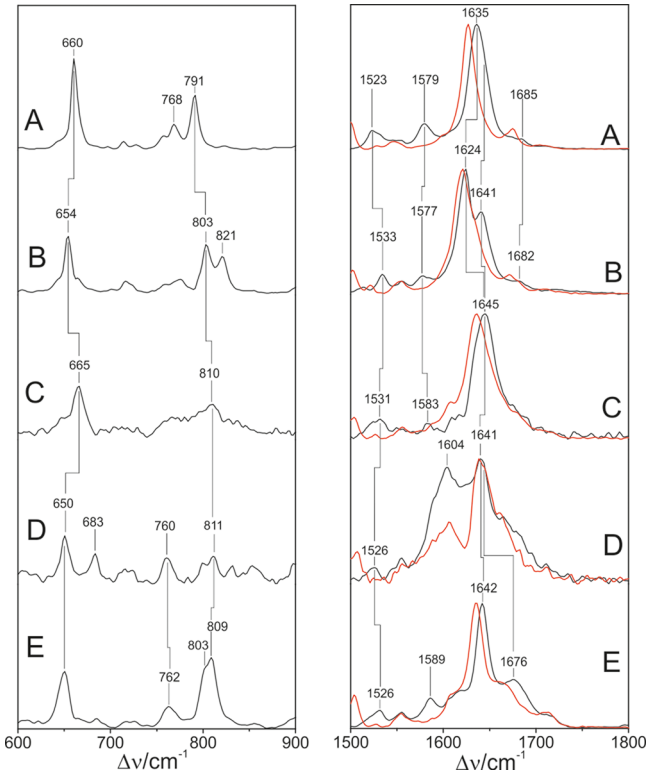

Figure 6. RR spectra of the species constituting the Pr-to-Pg reaction pathway. A, Pr; B, Lumi-R; C, Meta-R1; D, Meta-R2; and E, Pg. The intermediates were trapped at the temperatures indicated in Figure 5. The black and red lines refer to the measurements in H_2O and D_2O solutions, respectively (pH 7.8).

Specifically, the *C*−*D* stretching undergoes an 11 cm^{-1} downshift to 1626 cm^{-1}, which, albeit smaller than in phyA (−37 cm^{-1})[41] makes the *A*−*B* stretching mode visible at 1641 cm^{-1}, which is obscured by the prominent 1635 cm^{-1} band in the Pr spectrum. It is reasonable to assume that, like in phyA, the frequency of the *A*−*B* stretching mode is not significantly affected by the photoisomerization. In conjunction with the distinctly lower RR activity of the HOOP modes, the smaller downshift of the *C*−*D* stretching compared to that of phyA[41] may suggest that the cryogenically trapped Lumi-R represents an already partially relaxed state, consistent with the relatively slow formation kinetics. In addition, it may be that with the formation of Lumi-R, water molecules enter the chromophore binding pocket, thereby causing an upshift of the methine bridge stretching frequencies as discussed above (Supporting Information, Figures S4 and S5 and Table S3).

The subsequent formation of the intermediate Meta-R1 involves further thermal relaxation of the cofactor structure reflected by an even lower HOOP RR activity. In both the Lumi-R and the Meta-R1 state, the PCB chromophore is protonated as indicated by the protonation marker band (ring *B* and *C* N−H ip) at 1577 and 1583 cm^{-1}, respectively (Figure 6B,C). The situation is different for the following thermal relaxation product, Meta-R2 (Figure 6D), which is very similar

dx.doi.org/10.1021/bi400506a | *Biochemistry* 2013, 52, 4871−4880

to the Meta-Rc states identified in the photoconversion routes of phyA as well as those of PCB- and biliverdin-binding (cyano)bacterial phytochromes. Both the distinctly lower resonance enhancement, presumably due to the reduced oscillator strength of the first electronic transition, and the lack of the N−H ip mode and the unique broad and poorly resolved vibrational structure in the C=C stretching region are characteristic features of a protein complex carrying a nonprotonated (neutral) tetrapyrrole cofactor.[41,47,48]

The photoinduced transformation from Pg back to Pr runs via three intermediates that can be cryogenically trapped (Figure 5). Unlike the forward reaction (Pr-to-Pg), formation of the first intermediate Lumi-G was already observed at −140 °C, although a better trapping yield is obtained at −120 °C. These findings imply that the (thermal) activation barrier is much lower than for the Lumi-R formation, again consistent with previous kinetic studies.[30] Most surprisingly, the RR spectrum of Lumi-G displays a broad envelope in the C=C stretching region with maxima at ca. 1645 and 1675 cm^{-1} that are similar in frequency as the well-defined peaks of the parent Pg state (Figure 7A,B). It may be that this band contour

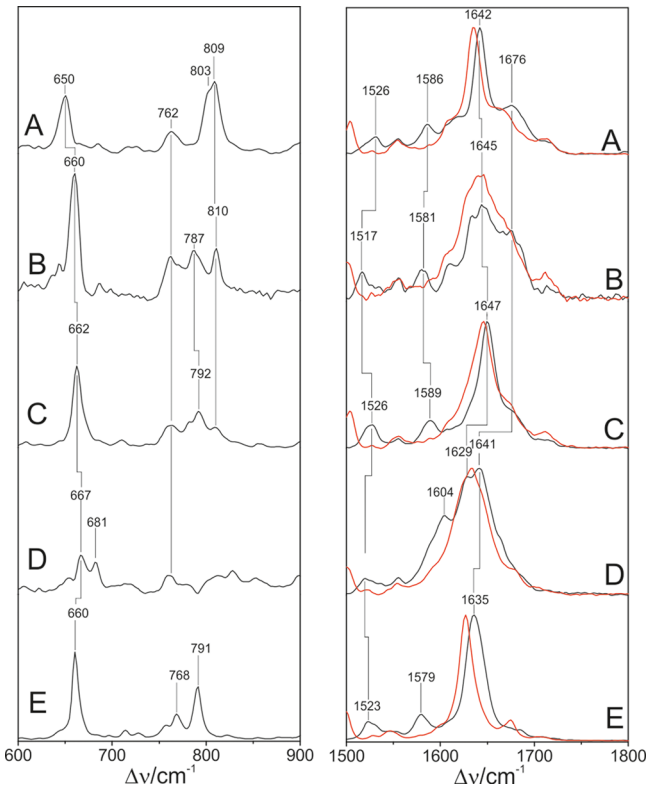

Figure 7. RR spectra of the species constituting the Pg-to-Pr reaction pathway. A, Pg; B, Lumi-G; C, Meta-G1; D, Meta-G2; and E, Pr. The intermediates were trapped at the temperatures indicated in Figure 5. The black and red lines refer to the measurements in H_2O and D_2O solutions, respectively (pH 7.8).

represents the overlapping contributions of more than one intermediate containing a largely distorted *ZZZssa* configuration; however, the poor signal-to-noise ratio impairs precise identification of the individual band components. Also, the HOOP region displays a rather complex but well-resolved vibrational band pattern. It is therefore interesting to note that for the reverse reaction of another phytochrome-like protein, bacteriochrome NpR6012g4, two subsequent Lumi-G intermediates were detected.[49] Assuming a similar reaction pathway for AnPixJg2, the present RR spectrum is interpreted as a mixture of two Lumi-G species, which are trapped between −140 and −120 °C. During the thermal relaxation from Lumi-G to Meta-G1 (Figure 7C), the chromophore is converted into a less distorted conformation as indicated by rather sharp bands in the C=C stretching and the low RR activity in the HOOP region. Like in Lumi-G, the PCB cofactor is protonated, as shown by the N−H ip mode at 1586 cm^{-1}.

At −40 °C, the Meta-G2 intermediate is trapped as the precursor of the Pr state (Figure 7D). Meta-G2 shows spectral similarities to its counterpart of the Pr-to-Pg pathway. Meta-G2 and Meta-R2 display two broad peaks at 1604 and 1641 cm^{-1} (Figures 6D and 7D). Taking into account that the cofactor configurations must be different, i.e., *ZZEssa* and *ZZZssa* in Meta-R2 and Meta-G2, respectively, this spectral similarity seems to be surprising. However, previous studies on tetrapyrrole model compounds have shown that the spectral differences between double bond isomers of deprotonated (neutral) bilins are rather small.[50] Interestingly, a band to be attributed to the N−H ip mode of rings *B* and *C* cannot be identified, implying that also in Meta-G2 the cofactor is deprotonated.

Structural and Mechanistic Similarities to Classical Phytochromes. The second GAF domain of the cyanobacteriochrome AnPixJg2 carries a PCB cofactor that undergoes photoinduced reaction cascades very similar to those in canonical phytochromes. The phototransformations between the parent states Pr and Pg are initiated by a photoisomerization of the *C*−*D* methine bridge double bond, followed by thermal reaction steps, including relaxation processes of the chromophore and chromophore−protein interactions, and eventually leading to a reversible deprotonation of the cofactor. The present MD simulations point to a significant increase of the solvent accessible area in the "photoproduct" model, accompanied by an increase of the number of water molecules in the cofactor pocket (vide supra). Concomitant to the rupture of the Trp90−PCB interactions, the protein adopts a more "open" structure, allowing for an exchange of water molecules between the chromophore pocket and the solution phase. Although a 15 ns MD simulation is not appropriate to deliver a reliable model for a protein state formed on the microsecond time scale, the present simulation suggests that cofactor structural changes may in fact serve as a switch to enable proton translocation through the protein. It remains to be explored in future experiments whether this proton transfer is associated with a transient proton release to the solution phase as shown for Cph1[51] and Agp1.[47] In these classical phytochromes, the proton translocation appears to serve as a trigger for protein conformational changes that may represent the signaling event.[47]

Altogether, we conclude that essential steps of the reaction pattern of classical phytochromes are also found in the CBRC AnPixJg2. This is also true for the considerable structural heterogeneity of the cofactor in the Pg state which may be compared to the substate equilibria in the Pfr state of prototypical phytochromes.[44] In the latter case, this conformational equilibrium was suggested to facilitate the dark conversion from the Pfr to the Pr state, in contrast to the thermally stable Pfr state of bathy phytochromes.[44] In fact, a slow Pg → Pr dark conversion is also noted for AnPixJg2.

Color Tuning in the Cyanobacteriochrome AnPixJg2. The most striking difference between AnPixJg2 and canonical

dx.doi.org/10.1021/bi400506a | *Biochemistry* 2013, 52, 4871−4880

phytochromes refers to the unusually blue-shifted absorption of the Pg parent state, the counterpart of the far-red-absorbing Pfr state of classical phytochromes. This blue shift is accompanied by large frequency upshifts of all methine bridge stretchings, even the structurally rather insensitive *B*−*C* stretching, and also of the N−H ip mode. These systematic frequency upshifts cannot be related to ground state structural changes of the cofactor (vide supra) but are instead, together with the hypsochromically shifted electronic absorption, reminiscent of the so-called opsin shift in (bacterial) rhodopsins carrying a protonated retinal Schiff base as a cofactor.[52] Here, the specific cofactor−protein interactions have been shown to perturb the energy levels of the highest occupied and lowest unoccupied molecular orbitals such that the excitation energy of the first electronic transition may vary substantially, covering a range of absorption maxima from 600 to 400 nm. These changes in the absorption maxima are inversely related to the frequency of the C=C stretching modes of the polyene chain. These tendencies nicely match the observations for the Pg and Pfr states of AnPixJg2 and canonical phytochromes, respectively. Whereas in AnPixJg2, the hypsochromic shift of the absorption maximum in Pg compared to Pr is accompanied by an upshift of the C=C stretching frequencies, the opposite shifts of the absorption maxima and the C=C stretching frequencies are observed for the Pr → Pfr transition in canonical phytochromes.

The factors controlling the opsin shift in retinal proteins have been extensively studied in the past decades, and it was demonstrated that both electrostatic and hydrophobic interactions may be responsible for tuning the energy levels.[52] These interactions may be accomplished by the appropriate positioning of charged, polar, and unpolar amino acid side chains in the vicinity of the chromophore. Alternatively, also an increased solvent (water) exposure may cause a significant blue shift of the absorption maximum and the corresponding upshift of the C=C stretchings as revealed by the comparison of protonated retinal Schiff bases in protic solvents and in the protein-embedded state.[53] Although rearrangements of charged and uncharged amino acids in the chromophore binding pocket cannot be ruled out for the Pr → Pg transition of AnPixJg2, a significant increase of the solvent accessibility is likely to occur as suggested by the present MD simulations of the Pg model. Thus, we conclude that the influx of water molecules into the chromophore binding pocket is the main origin for the shifts of the electronic energy levels which raise the energy of the first electronic transition, concomitant to upshifts of the methine bridge stretching frequencies.

According to the MD simulations, the cofactor photoisomerization initiates the increase of solvent accessibility of the chromophore. This interpretation is consistent with the RR spectroscopic data. Because AnPixJg2 and canonical phytochromes seem to exhibit very similar cofactor structures in the corresponding states of the Pr → Pg(Pfr) forward and backward transformations, the additional frequency shifts suggest a stepwise influx of water into the chromophore binding pocket in AnPixJg2 during the formation of the Lumi-R (Lumi-F) photoproduct and the recovery of the final state Pg(Pr) (see Supporting Information, Figures S4 and S5 and Table S3).

In summary, AnPixJg2 seems to employ a unique strategy for color tuning that is different from those in other CBCRs. Instead of acid/base reactions for de- and reprotonating the cofactor, or chemical modifications via Cys side chains to perturb the π-electron systems,[17,21−23,54] the PCB cofactor in AnPixJg2 remains protonated and adopts a conformation very similar to that of its Pfr counterpart in canonical phytochromes. In AnPixJg2, the substantial color change is instead attributed to a strongly increased solvent accessibility, which is the result of the altered cofactor−protein (PCB−Trp90) interactions initiated by the *Z* → *E* isomerization of the chromophore. Presumably, such a mechanism for color tuning is possible only because of the small size of the "GAF-only" protein compared to classical PAS-GAF-PHY phytochromes.

■ ASSOCIATED CONTENT

Supporting Information

Additional experimental details and RR spectra, including a description of the subtraction procedure, an analysis of the solvent effects on the RR spectra, and further figures and tables illustrating the MD simulation. This material is available free of charge via the Internet at http://pubs.acs.org.

■ AUTHOR INFORMATION

Corresponding Author

*Tel: +49-30-314-21419. Fax: +49-30-314-21122. E-mail: Hildebrandt@chem.tu-berlin.de.

Funding

The work was supported by Deutsche Forschungsgemeinschaft, Sfb1078 (B6, C3).

Notes

The authors declare no competing financial interest.

■ ACKNOWLEDGMENTS

The authors thank the "Norddeutscher Verbund für Hoch- und Höchstleistungsrechnen" (HLRN) for providing computer power.

■ ABBREVIATIONS

Agp1 and Agp2, *Agrobacterium tumefaciens* phytochromes 1 and 2, respectively; *a* and *s*, nomenclature for the methine bridge single bond conformation (*anti* and *syn*, respectively); CBCR, cyanobacteriochrome; Cph1, cyanobacterium *Synechocystis* sp. PCC 6803 phytochrome 1; EDTA, ethylenediaminetetraacetic acid; GAF, cGMP specific phosphodiesterases, adenylate cyclases, formate hydrogen lyase transcription activator; HOOP, hydrogen-out-of-plane; MD, molecular dynamics; Nd:YAG, neodymium-doped yttrium aluminum garnet; N−H ip, N−H in plane bending vibrational mode; Pap1, *Pseudomonas aeruginosa* phytochrome 1; PAS, PER/ARNT/SIM protein domain; PCB, phycocyanobilin; Pfr, phytochrome far-red-absorbing form; PHY, phytochrome specific domain; phyA−phyE, plant phytochromes A−E from *A. thaliana*; Pg and Pr, green- and red-absorbing form of the pigment, respectively; PVB, phycoviolobilin; RR, resonance Raman; TePixJ, PixJ of *Thermosynechococcus elongatus* GAF-only blue/green-absorbing cyanobacteriochrome; Tris, tris-(hydroxymethyl)aminomethane; *Z* and *E*, nomenclature for the methine bridge double bond configuration (*Zusammen* and *Entgegen*, respectively, corresponding to *cis/trans*)

■ REFERENCES

(1) Butler, W. L., Norris, K. H., Siegelman, H. W., and Hendricks, S. B. (1959) Detection, assay, and preliminary purification of the pigment controlling photoresponsive development of plants. *Proc. Natl. Acad. Sci. U.S.A. 45*, 1703−1708.

(2) Siegelman, H. W., and Firer, E. M. (1964) Purification of phytochrome from oat seedlings. *Biochemistry 3*, 418−423.
(3) Kendrick, R. E., and Kronenberg, G. H. M. (1994) *Photomorphogenesis in Plants*, Kluwer Academic Publishers, Dordrecht, The Netherlands.
(4) Whitelam, G. C., Patel, S., and Devlin, P. F. (1998) Phytochromes and photomorphogenesis in *Arabidopsis*. *Philos. Trans. R. Soc., B 353*, 1445−1453.
(5) Neff, M., Fankhauser, C., and Chory, J. (2000) Light: An indicator of time and place. *Genes Dev. 14*, 257−271.
(6) Casal, J. J., Luccioni, L. G., Oliverio, K. A., and Boccalandro, H. E. (2003) Phytochrome signaling and photomorphogenesis in *Arabidopsis*. *Photochem. Photobiol. Sci. 2*, 625−636.
(7) Butler, W. L. (1972) in *Phytochrome* (Mitrakos, M., and Shropshire, W., Eds.) pp 182−192, Academic Press, New York.
(8) Kendrick, R. E., and Spruit, C. J. P. (1977) Phototransformations of phytochrome. *Photochem. Photobiol. 26*, 201−214.
(9) Rüdiger, W. (1992) Events in the phytochrome molecule after irradiation. *Photochem. Photobiol. 56*, 803−809.
(10) Sineshchekov, V. A. (1995) Photobiophysics and photobiochemistry of the heterogeneous phytochrome system. *Biochim. Biophys. Acta 1228*, 125−164.
(11) Braslavsky, S. E., Gärtner, W., and Schaffner, K. (1997) Phytochrome photoconversion. *Plant Cell Environ. 20*, 700−706.
(12) Braslavsky, S. E. (2003) in *Photochromism, Molecules and Systems* (Bouas-Laurent, D., and Bouas-Laurent, H., Eds.) pp 738 − 755, Elsevier Science, Amsterdam.
(13) Mroginski, M., von Stetten, D., Kaminski, S., Velazquez Escobar, F., Michael, N., Daminelli-Widany, G., and Hildebrandt, P. (2011) Elucidating photoinduced structural changes in phytochromes by the combined application of resonance Raman spectroscopy and theoretical methods. *J. Mol. Struct. 993*, 15−25.
(14) Hughes, J., Lamparter, T., Mittmann, F., Hartmann, E., Gärtner, W., Wilde, A., and Börner, T. (1997) A prokaryotic phytochrome. *Nature 386*, 663−663.
(15) Karniol, B., Wagner, J. R., Walker, J. M., and Vierstra, R. D. (2005) Phylogenetic analysis of the phytochrome superfamily reveals distinct microbial subfamilies of photoreceptors. *Biochem. J. 392*, 103−116.
(16) Karniol, B., and Vierstra, R. D. (2003) The pair of bacteriophytochromes from *Agrobacterium tumefaciens* are histidine kinases with opposing photobiological properties. *Proc. Natl. Acad. Sci. U.S.A. 100*, 2807−2812.
(17) Hirose, Y., Rockwell, N. C., Nishiyama, K., Narikawa, R., Ukajic, Y., Inomata, K., Lagarias, J. C., and Ikeuchi, M. (2013) Green/red cyanobacteriochromes regulate complementary chromatic acclimation via a protochromic photocycle. *Proc. Natl. Acad. Sci. U.S.A. 110*, 4974−4979.
(18) Ikeuchi, M., and Ishizuka, T. (2008) Cyanobacteriochromes: A new superfamily of tetrapyrrole-binding photoreceptors in cyanobacteria. *Photochem. Photobiol. Sci. 7*, 1159−1167.
(19) Rockwell, N. C., and Lagarias, J. C. (2010) A brief history of phytochromes. *ChemPhysChem 11*, 1172−1180.
(20) Song, J.-Y., Cho, H. S., Cho, J. I., Jeon, J.-S., Lagarias, J. C., and Park, J. I. (2011) Near-UV cyanobacteriochrome signaling system elicits negative phototaxis in the cyanobacterium *Synechocystis sp. PCC 6803*. *Proc. Natl. Acad. Sci. U.S.A. 108*, 10780−1785.
(21) Ulijasz, A. T., Cornilescu, G., von Stetten, D., Cornilescu, C., Velazquez Escobar, F., Zhang, J., Stankey, R. J., Rivera, M., Hildebrandt, P., and Vierstra, R. D. (2009) Cyanochromes are blue/green light photoreversible photoreceptors defined by a stable double cysteine linkage to a phycoviolobilin-type chromophore. *J. Biol. Chem. 284*, 29757−29772.
(22) Rockwell, N. C., Njuguna, S. L., Roberts, L., Castillo, E., Parson, V. L., Dwojak, S., Lagarias, J. C., and Spiller, S. C. (2008) A second conserved GAF domain cysteine is required for the blue/green photoreversibility of cyanobacteriochrome Tlr0924 from *Thermosynechococcus elongates*. *Biochemistry 47*, 7304−7316.
(23) Ishizuka, T., Kamiya, A., Suzuki, H., Narikawa, R., Noguchi, T., Kohchi, T., Inomata, K., and Ikeuchi, M. (2011) The cyanobacteriochrome, TePixJ, isomerizes its own chromophore by converting phycocyanobilin to phycoviolobilin. *Biochemistry 50*, 953−961.
(24) Ulijasz, A. T., Cornilescu, G., Cornilescu, C. C., Zhang, J., Rivera, M., Markley, J. L., and Vierstra, R. D. (2010) Structural basis for the photoconversion of a phytochrome to the activated Pfr form. *Nature 463*, 250−254.
(25) Kaminski, S., and Mroginski, M. A. (2010) Molecular dynamics of phycocyanobilin binding bacteriophytochromes: A detailed study of structural and dynamic properties. *J. Phys. Chem. B 114*, 16677−16686.
(26) Kneip, C., Hildebrandt, P., Nemeth, K., Mark, F., and Schaffner, K. (1999) Interpretation of the resonance Raman spectra of linear tetrapyrroles based on DFT calculations. *Chem. Phys. Lett. 311*, 479−484.
(27) Mroginski, M. A., von Stetten, D., Velazquez Escobar, F., Strauss, H. M., Kaminski, S., Scheerer, P., Günther, M., Murgida, D. H., Schmieder, P., Bongards, C., Gärtner, W., Mailliet, J., Hughes, J., Essen, L.-O., and Hildebrandt, P. (2009) Chromophore structure of cyanobacterial phytochrome Cph1 in the Pr state: Reconciling structural and spectroscopic data by QM/MM calculations. *Biophys. J. 96*, 4153−4163.
(28) Narikawa, R., Fukushima, Y., Ishizuka, T., Itoh, S., and Ikeuchi, M. (2008) A novel photoactive GAF domain of cyanobacteriochrome AnPixJ that shows reversible green/red photoconversion. *J. Mol. Biol. 380*, 844−855.
(29) Narikawa, R., Ishizuka, T., Muraki, N., Shiba, T., Kurisu, G., and Ikeuchi, M. (2013) Structures of cyanobacteriochromes from phototaxis regulators AnPixJ and TePixJ reveal general and specific photoconversion mechanism. *Proc. Natl. Acad. Sci. U.S.A. 110*, 918−923.
(30) Fukushima, Y., Iwaki, M., Narikawa, R., Ikeuchi, M., Tomita, Y., and Itoh, S. (2011) Photoconversion mechanism of a green/red photosensory cyanobacteriochrome AnPixJ: Time-resolved optical spectroscopy and FTIR analysis of the AnPixJ-GAF2 domain. *Biochemistry 50*, 6328−6339.
(31) Joergensen, W. L., Chandrasekhar, J., Madura, J. D., Impey, R. W., and Klein, M. L. (1983) Comparison of simple potential functions for simulating liquid water. *J. Chem. Phys. 79*, 926−935.
(32) Phillips, J. C., Braun, R., Wang, W., Gumbart, J., Tajkhorshid, E., Villa, E., Chipot, C., Skeel, R. D., Kalé, L., and Schulten, K. (2005) Scalable molecular dynamics with NAMD. *J. Comput. Chem. 26*, 1781−1802.
(33) MacKerell, A. D., Bashford, D., Bellott, M., Dunbrack, R. L., Jr., Evanseck, J. D., Field, M. J., Fischer, S., Gao, J., Guo, H., Ha, S., Joseph-McCarthy, D., Kuchnir, L., Kuczera, K., Lau, F. T. K., Mattos, C., Michnick, S., Ngo, T., Nguyen, D. T., Prodhom, B., Reiher, W. E., III, Roux, B., Schlenkrich, M., Smith, J. C., Stote, R., Straub, J., Watanabe, M., Wiórkiewicz-Kuczera, J., Yin, D., and Karplus, M. (1998) All-atom empirical potential for molecular modeling and dynamics studies of proteins. *J. Phys. Chem. B 102*, 3586−3616.
(34) Kaminski, S., Daminelli-Widany, G., and Mroginski, M. A. (2009) Molecular dynamics simulations of the chromophore binding site of *Deinococcus radiodurans* bacteriophytochrome using new force field parameters for the phytochromobilin chromophore. *J. Phys. Chem. B 113*, 945−958.
(35) Feller, S. E., Zhang, Y., Pastor, R. W., and Brooks, B. R. (1995) Constant pressure molecular dynamics simulation: The Langevin piston method. *J. Chem. Phys. 103*, 4613−4621.
(36) Darden, T., York, D., and Pedersen, L. (1993) Particle mesh Ewald: An $N\cdot\log(N)$ method for Ewald sums in large systems. *J. Chem. Phys. 98*, 10089−10092.
(37) van Gunsteren, W., and Berendsen, H. (1977) Algorithms for macromolecular dynamics and constraint dynamics. *Mol. Phys. 34*, 1311−1327.
(38) Humphrey, W., Dalke, A., and Schulten, K. (1996) VMD: Visual molecular dynamics. *J. Mol. Graphics 14*, 33−38.

(39) Essen, L.-O., Mailliet, J., and Hughes, J. (2008) The structure of a complete phytochrome sensory module in the Pr ground state. *Proc. Natl. Acad. Sci. U.S.A. 105*, 14709−14714.
(40) Mroginski, M. A., Kaminski, S., von Stetten, D., Ringsdorf, S., Gärtner, W., Essen, L. O., and Hildebrandt, P. (2011) The structure of the chromophore binding pocket in the Pr state of plant phytochrome phyA. *J. Phys. Chem. B 115*, 1220−1231.
(41) Kneip, C., Hildebrandt, P., Schlamann, W., Braslavsky, S. E., Mark, F., and Schaffner, K. (1999) Protonation state and structural changes of the tetrapyrrole chromophore during the $P_r \rightarrow P_{fr}$ phototransformation of phytochrome: A resonance Raman spectroscopic study. *Biochemistry 38*, 15185−15192.
(42) Schwinté, P., Foerstendorf, H., Gärtner, W., Mroginski, M. A., Hildebrandt, P., and Siebert, F. (2008) Fourier transform infrared studies of the photoinduced processes of phytochrome phyA using isotopically labelled chromophores and density functional theory calculations. *Biophys. J. 95*, 1256−1267.
(43) Mroginski, M. A., Murgida, D. H., von Stetten, D., Kneip, C., Mark, F., and Hildebrandt, P. (2004) Determination of the chromophore structures in the photoinduced reaction cycle of phytochrome. *J. Am. Chem. Soc. 126*, 16734−16735.
(44) Salewski, J., Velazquez Escobar, F., Kaminski, S., von Stetten, D., Keidel, A., Rippers, Y., Michael, N., Scheerer, P., Piwowarski, P., Bartl, F., Frankenberg-Dinkel, N., Ringsdorf, S., Gärtner, W., Lamparter, T., Mroginski, M. A., and Hildebrandt, P. (2013) The structure of the biliverdin cofactor in the Pfr state of bathy and prototypical phytochromes. *J. Biol. Chem. 288*, 16800−16814.
(45) Wagner, J. R., Brunzelle, J. S., Forest, K. T., and Vierstra, R. D. (2005) A light-sensing knot revealed by the structure of the chromophore-binding domain of phytochrome. *Nature 438*, 325−331.
(46) Kim, P. W., Freer, L. H., Rockwell, N. C., Martin, S. S., Lagarias, J. C., and Larsen, D. S. (2012) Femtosecond photodynamics of the red/green cyanobacteriochrome NpR6012g4 from *Nostoc punctiforme*. 1. Forward dynamics. *Biochemistry 51*, 608−618.
(47) Borucki, B., von Stetten, D., Seibeck, S., Lamparter, T., Michael, N., Mroginski, M. A., Otto, H., Murgida, D. H., Heyn, M. P., and Hildebrandt, P. (2005) Light-induced proton release of phytochrome is coupled to the transient deprotonation of the tetrapyrrole chromophore. *J. Biol. Chem. 280*, 34358−34364.
(48) Von Stetten, D., Seibeck, S., Michael, N., Scheerer, P., Mroginski, M. A., Murgida, D. H., Krauss, N., Heyn, M. P., Hildebrandt, P., Borucki, B., and Lamparter, T. (2007) Highly conserved residues D197 and H250 in Agp1 phytochrome control the proton affinity of the chromophore and Pfr formation. *J. Biol. Chem. 282*, 2116−2123.
(49) Kim, P. W., Freer, L. H., Rockwell, N. C., Martin, S. S., Lagarias, J. C., and Larsen, D. S. (2012) Femtosecond photodynamics of the red/green cyanobacteriochrome NpR6012g4 from *Nostoc punctiforme*. 2. Reverse dynamics. *Biochemistry 51*, 619−630.
(50) Matysik, J., Hildebrandt, P., Smit, K., Mark, F., Gärtner, W., Braslavsky, S. E., Schaffner, K., and Schrader, B. (1997) Raman spectroscopic analysis of isomers of biliverdin dimethyl ester. *J. Pharm. Biomed. Anal. 15*, 1319−1324.
(51) van Thor, J. J., Borucki, B., Crielaard, W., Otto, H., Lamparter, T., Hughes, J., Hellingwerf, K. J., and Heyn, M. P. (2001) Light-induced proton release and proton uptake reactions in the cyanobacterial phytochrome Cph1. *Biochemistry 40*, 11460−11471.
(52) Lin, S. W., Kochendoerfer, G. G., Carroll, K. S., Wang, D., Mathies, R. A., and Sakmar, T. P. (1998) Mechanisms of spectral tuning in blue cone visual pigments. Visible and Raman spectroscopy of blue-shifted rhodopsin mutants. *J. Biol. Chem. 273*, 24583−24591.
(53) Nielsen, M. B. (2009) Model systems for understanding absorption tuning by opsin proteins. *Chem. Soc. Rev. 38*, 913−924.
(54) Enomoto, G., Hirose, Y., Narikawa, R., and Ikeuchi, M. (2012) Thiol-based photocycle of the blue and teal light-sensing cyanobacteriochrome Tlr999. *Biochemistry 51*, 3050−3058.